The preparation of highly dispersed Au/Al_2O_3 by aqueous impregnation

Qing Xu [a,*], Karl C.C. Kharas [b], and A.K. Datye [a]

[a] *Department of Chemical & Nuclear Engineering and Center for Microengineered Materials, University of New Mexico, Albuquerque, NM 87131, USA*

[b] *Delphi Catalyst, PO Box 580970, Tulsa, OK 74158-0970, USA*

Received 26 August 2002; accepted 7 November 2002

In this work, we report an impregnation method for preparing Au supported on alumina from $HAuCl_4$. In the literature, impregnation under acidic conditions has been found to lead to poor dispersions of Au and the resulting catalysts are not as active as those prepared by deposition–precipitation. To overcome these problems, we have developed a two-step procedure: in the first step, the acidified Au solution is contacted with alumina to adsorb the Au chloride on the alumina. After washing off the excess Au precursor, we treat the solid with a strong base to convert the chloride to an absorbed hydroxide. Drying and calcination at 400 °C yields a catalyst with Au particles having a number average diameter of 2.4 nm. The reactivity for CO oxidation at room temperature is comparable to catalysts prepared by deposition–precipitation. These catalysts are stable to hydrothermal sintering, with average particle size around 4 nm after sintering in 10 mol% H_2O at 600 °C for 100 h. This work shows that stable Au/Al_2O_3 catalysts having a high reactivity for CO oxidation can be prepared by impregnation under acidic conditions.

KEY WORDS: gold dispersion; aqueous impregnation of gold.

1. Introduction

Gold is generally regarded as the least useful of the noble metals for catalytic purposes. The low activity of gold is due to a filled *d*-band, with the result that gold is unable to chemisorb small molecules [1]. Interest in Au catalysts was sparked by the work of Haruta *et al.* [2] who showed that very finely divided gold particles supported on transition metal oxides are very active for CO oxidation, even at temperatures as low as −70 °C. Such small metal crystallites become electron deficient, and their properties then resemble those of the preceding element in the Periodic Table, so that very finely divided gold particles take on some of the properties of platinum metal [1,3]. The nature of the active sites, and the cause of catalytic activity in Au, is still disputed, and is a subject of intense study. However, one aspect of Au catalysis is not disputed: that Au particles in the size range 2–3 nm show high activity for CO oxidation. Our work is directed at methods of preparing such catalysts and improving their hydrothermal stability. Gold catalysts containing nanoparticles are able to catalyze many reactions under conditions where bulk metallic gold is inactive.

The method that reportedly yields the best dispersion of Au nanoparticles, and the most active catalysts, is deposition–precipitation (DP) [4]. Deposition–precipitation from $HAuCl_4$ is typically carried out over a pH range of 6–10. Catalysts prepared at lower pH values are generally less active, due to the presence of residual chloride, which acts as a poison and leads to sintering of the Au particles, as suggested by the recent work of Oh *et al.* [5]. In their study, the most active catalysts were prepared by the deposition–precipitation method at pH 7 and a temperature of 70 °C. The only report of the use of impregnation to prepare high-activity catalysts is with Au organophosphine precursors, as reported by the Iwasawa group [6]. However, impregnation by the commonly available $HAuCl_4$ precursor would be the method most amenable to scaling up for industrial manufacture. With this in mind, we have developed a procedure that allows us to use acidified gold precursor solutions followed by a washing step under basic conditions. Using this approach, we can maintain high dispersions of Au and a further advantage is that these catalysts are stable against sintering at elevated temperature. The activity of these catalysts compares favorably with the best catalysts reported in the literature. As we show in this paper, the key step is the removal of chloride ion impurities after the impregnation step, a step which is not usually performed during conventional impregnation.

2. Experimental

The catalyst was prepared using SCCa90 alumina obtained from Condea Vista Company (now Sasolchemie GmbH). This phase is primarily θ alumina with

* To whom correspondence should be addressed.

1011-372X/03/0200-0229/0

a BET surface area of about $90\,m^2/g$. A slurry of this alumina was prepared by adding 30 g of alumina into 200 ml of deionized water. Into this slurry we added dropwise 10.8 ml of an acidified solution (density $\sim$1.4 g/ml) containing 19.68 wt% $HAuCl_4$, with stirring for 1 h. During this step, the alumina adsorbed some of the gold precursor and took on a yellowish color. The supernatant liquid was decanted and the solid was washed five times with deionized water. The solid was then contacted with an aqueous solution of $NH_3 \cdot H_2O$ until the pH did not change any more. During this step, the Au chloride adsorbed on the support was converted into a hydroxide. The mixture was then washed again five times with deionized water, dried at 100 °C overnight and calcined in air at 400 °C for 4 h. After calcination, the catalyst developed a brown color. The metal loading achieved with this procedure was 1 wt% Au, as measured by atomic absorption spectroscopy. XRD showed no gold peaks after the calcination step. Two additional catalysts were prepared by using lower concentrations of the gold chloride to obtain lower loading of Au. Activity data are also reported for these catalysts which have 0.25 and 0.19 wt% Au.

High-resolution TEM was performed using a JEOL 2010F microscope operating at 200 kV and with a point resolution of 0.18 nm in TEM mode as well as in STEM HAADF mode. The TEM images showed that the gold particles were evenly dispersed on the support with an average diameter of about 2.3 nm. Due to the small particle size and the contrast from the alumina support, the best images were obtained during high-angle annular dark-field (HAADF) imaging in the STEM mode. The catalyst was sintered at 600 and 900 °C in N_2 with 10% H_2O for up to 96 h using the procedure described elsewhere [7], which involves quenching the catalyst in liquid nitrogen at the end of the sintering step to prevent any oxidation during cooling.

The reactivity in CO oxidation was measured using a fixed-bed microreactor consisting of a quarter-inch outer diameter stainless U-tube. The catalyst was retained in quartz wool, and a thermocouple was inserted into the bed to record the temperature. Since CO oxidation is an exothermic reaction, we found that the catalyst temperature would increase significantly as soon as the reactant flow was turned on. Hence, this U-tube reactor was immersed in a water bath to keep the catalyst at room temperature. The feed was nearly stoichiometric with a slight excess of O_2. The flow rates were 5.9 sccm of O_2, 11.4 sccm of CO and 40 sccm of He. The CO was purified by passing it through a bed of alumina spheres heated to 300 °C to decompose any carbonyls in the feed stream. The reaction mixture leaving the reactor was analyzed with an on-line gas chromatograph equipped with a TCD detector. About 0.05 g of catalyst sample was used. Reactor effluent concentrations were measured every 20 min.

3. Results

3.1. TEM analysis

Figure 1 shows a TEM image of the 1 wt% Au/Al_2O_3 catalyst after calcination at 400 °C. While the Au nanoparticles are well resolved, diffraction contrast from the alumina support makes it difficult to obtain good statistics. By switching to HAADF mode, contrast is now based on sample thickness and on atomic number. As seen in figure 2, Au particles are now imaged as bright objects on a dark background, making it possible

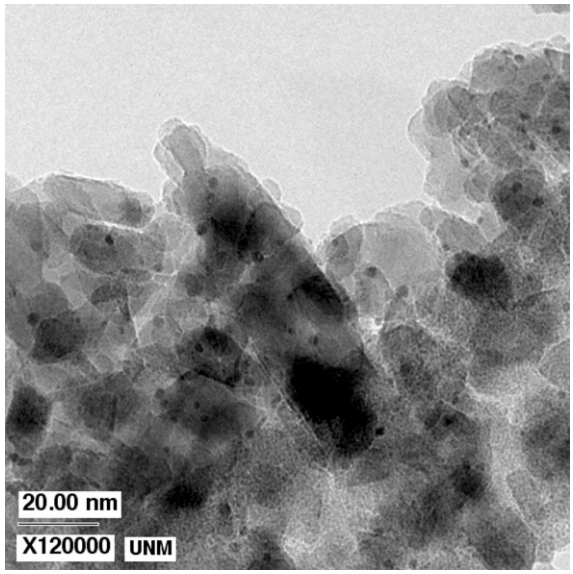

Figure 1. TEM image of 1 wt% Au/Al_2O_3. Small metal particles can be seen, but contrast from the support makes it difficult to image the Au nanoparticles.

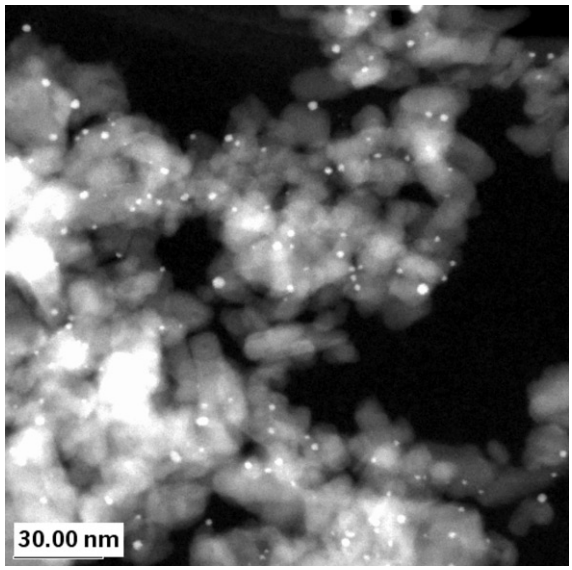

Figure 2. HAADF image of 1 wt% Au/Al_2O_3. Contrast is based on thickness and atomic number, making it easier to see a large number of metal particles. The average diameter is 2.1 nm.

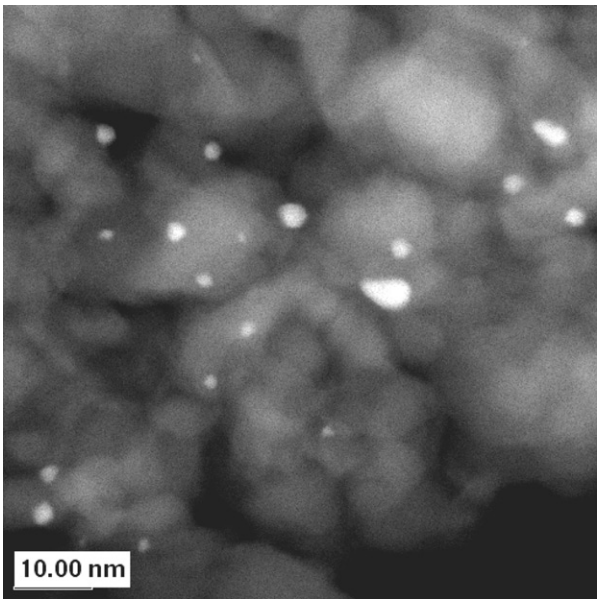

Figure 3. HAADF image of 1 wt% Au/Al_2O_3 catalyst after sintering in 10% H_2O/N_2 at 600 °C for 0 h (sample quenched as soon as temperature was reached). The number average diameter has increased to 2.6 nm.

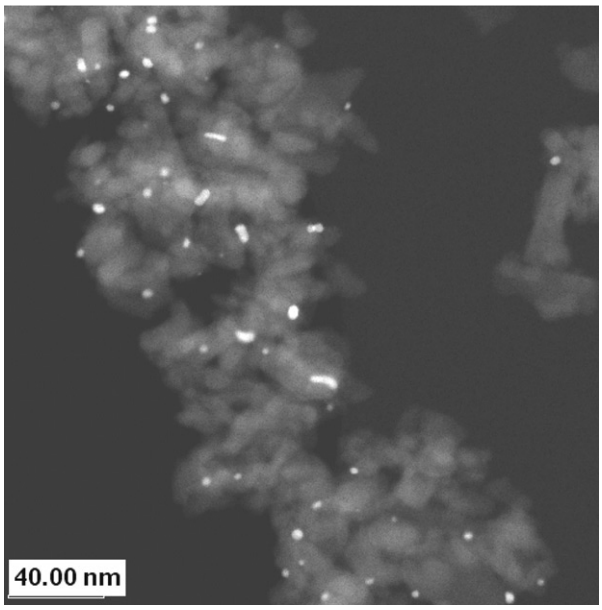

Figure 4. HAADF image of 1 wt% Au/Al_2O_3 catalyst after sintering in 10% H_2O/N_2 at 600 °C for 96 h. The number average diameter has increased to 4.1 nm and several elongated particles are seen suggestive of particle coalescence.

to see even the smallest Au particles very easily. The probe diameter during these imaging conditions is <0.2 nm, ensuring that probe convolution effects do not have to be considered. Figure 3 shows an image of the same catalyst after heating in flowing 10 mol% H_2O in N_2 at 600 °C for 0 h (the catalyst was quenched as soon as the temperature reached 600 °C). It is clear that some particles have grown in size, and there appear to be fewer particles in the vicinity of these larger particles. The elongated shapes of these larger particles are suggestive of coalescence as a cause of particle growth. The number average particle diameter has increased to 2.6 nm. Heating at 600 °C in the same atmosphere for 96 h leads to further growth of particles and clearer evidence of ellipsoidal particles, as seen in figure 4. The number average particle diameter has increased to 4.1 nm. Particle sizes of samples treated for different times were fitted very well by a log normal distribution, as shown in figures 5 and 6. The mean

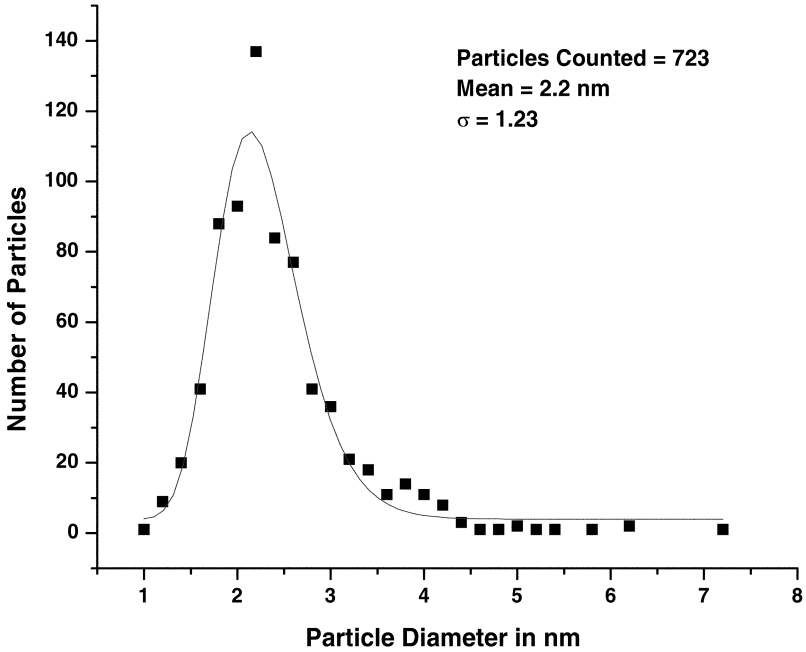

Figure 5. Particle size distribution of the 1 wt% Au/Al_2O_3 catalyst after initial calcination at 400 °C. This is the sample imaged in figures 1 and 2. The mean of 2.2 nm and σ of 1.2 are based on a log normal fit to the data.

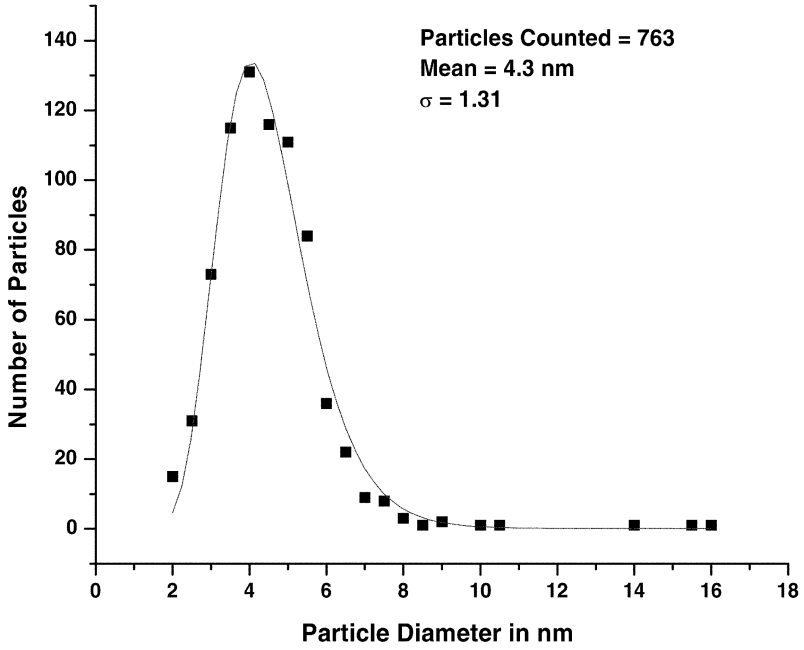

Figure 6. Particle size distribution of 1 wt% Au/Al_2O_3 after sintering in 10% H_2O/N_2 at 600 °C for 96 h. The mean diameter based on the log normal distribution has increased to 4.3 nm but σ is almost the same as the fresh catalyst.

diameter quoted in these figures is the geometric mean, as derived from the log normal fit.

Since the complete size distribution was determined, it was possible to obtain several other mean diameters, namely the surface average, volume average and perimeter average. To calculate dispersion, the particle shape was assumed to be spherical, and under these conditions the dispersion (fraction of surface atoms) is approximately equal to $1/D_s$. The various averages are reported in table 1, as also is the turnover frequency (TOF) based on the assumption that all surface atoms are active. The first three, D_n, D_s and D_v are well known in the literature, and defined elsewhere [7]. We have computed a perimeter average to test the assumption that catalyst activity resides in perimeter sites. The perimeter average is defined as the sum of the squares of the diameter divided by the sum of the diameters.

Table 1
Reactivity as a function of particle diameter [a]

	1% fresh	600 °C, 0 h	600 °C, 96 h	0.19% fresh	0.25% fresh
Reactivity	8.98	5.56	2.74	8.46	1.91
D_n	2.3	2.6	4.1	2.1	3.4
D_s	2.8	3.2	5.3	2.2	12.7
D_v	3.2	3.5	6.4	2.3	19.2
D_p	2.6	3.0	4.9	2.2	8.7
Dispersion $= 1/D_s$	0.36	0.31	0.19	0.45	0.08
TOF (s^{-1})	0.49	0.35	0.29	0.37	0.48

[a] Reactivity, moles CO_2/g Au/s $\times 10^4$ at room temperature; TOF, turnover frequency (reactivity $\times$ atomic wt of Au/dispersion); D_n, number average diameter; D_s, surface average; D_v, volume average; D_p, perimeter average.

Since the perimeter length per unit volume scales as $1/(D_p)^2$, we would expect reactivity to scale linearly with this quantity for a reaction that occurs only on perimeter sites. On the other hand, the surface area per unit volume scales as $(1/D_s)$, hence if all surface sites were active, the reactivity should scale linearly with this quantity.

3.2. CO oxidation activity

The Au catalysts were tested for CO oxidation after the initial calcinations at 400 °C (the fresh state). The 1 wt% catalyst was active for CO oxidation at room temperature. There was a drop in activity as the catalyst was exposed to the reactant gas, with the activity leveling off after a period of 100 min. As soon as the catalyst was exposed to the reactant gas, we observed a significant rise in temperature due to the exothermic CO oxidation reaction. This measurement was possible because of the thermocouple that was immersed into the catalyst bed. To ensure isothermal operation, we used a water bath to improve the heat transfer from the stainless steel reactor. Figure 7 shows the reactivity as a function of time using a water bath as the cooling medium for the fresh catalyst, as well as the catalysts sintered at 600 °C for 0 and 96 h. The extent of the temperature rise was much smaller with the sintered catalyst due to the lower activity. If we plot the data in figure 7 as a fraction of initial activity, the curves would be identical, suggesting that the mechanism responsible for the drop in activity is similar for all three catalysts. While some of the drop is caused by the decay in catalyst temperature with time, the loss of surface hydroxyls, as suggested

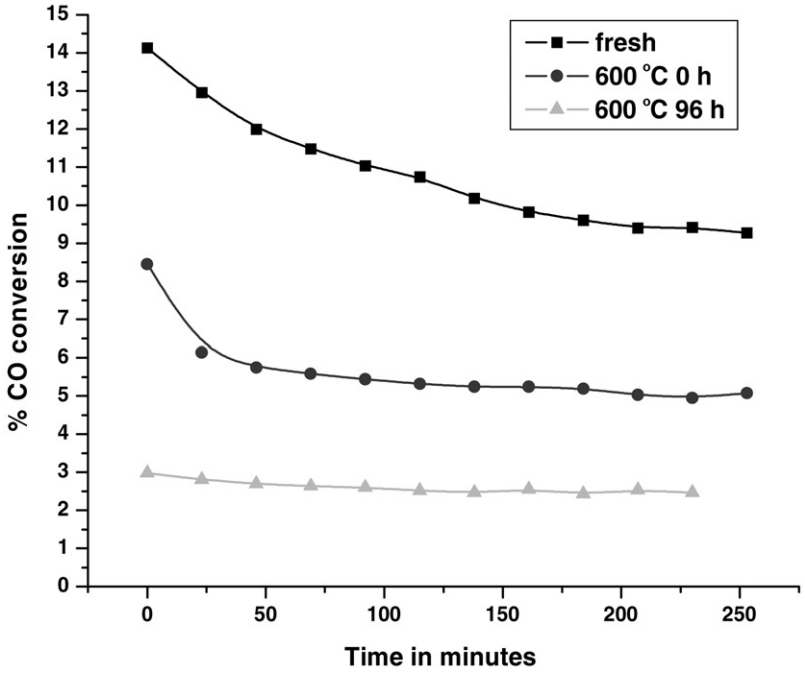

Figure 7. Conversion of CO at room temperature for the fresh and sintered 1 wt% Au/Al_2O_3 catalyst. The initial deactivation of these catalysts is not as pronounced with the sintered catalysts.

by Costello *et al*. [8], may also be responsible for the observed initial deactivation.

Figure 8 shows the Arrhenius plot for the fresh catalyst activity as a function of temperature. The observed apparent activation energy for the reaction was 17.0 kJ/mol. Haruta and Date [4] report that the activation energy varies with reaction temperature and ranges from near zero on metallic sites (steps and edges) to about 30 kJ/mol on perimeter sites. Our observed activation energy is within this range, and consistent with other reports in the literature [3]. We investigated the regeneration of this catalyst and found that flowing pure H_2 (figure 9) was able to reverse the drop in activity caused during the reaction period, similar to the observation by Costello *et al*. [8]. The variation in activity with average particle diameter is shown in figure 10. These results show that activity drops dramatically with increasing particle diameter. Since we have measured the particle size distribution, we are able to calculate the various averages which could be used to correlate reactivity with diameter. Figure 11 shows the test of two alternative models for catalyst reactivity (surface sites versus perimeter sites). If catalyst activity were to reside exclusively on surface sites, we would expect the activity to vary linearly with $(1/D_s)$, where D_s is the surface average diameter.

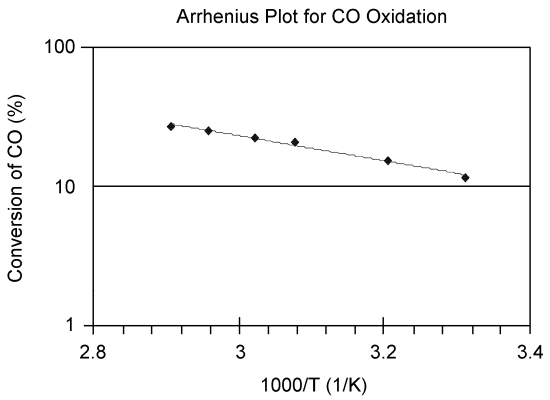

Figure 8. Arrhenius plot for CO oxidation on the fresh 1 wt% Au/Al_2O_3 catalyst. The activation energy is 17 kJ/mol.

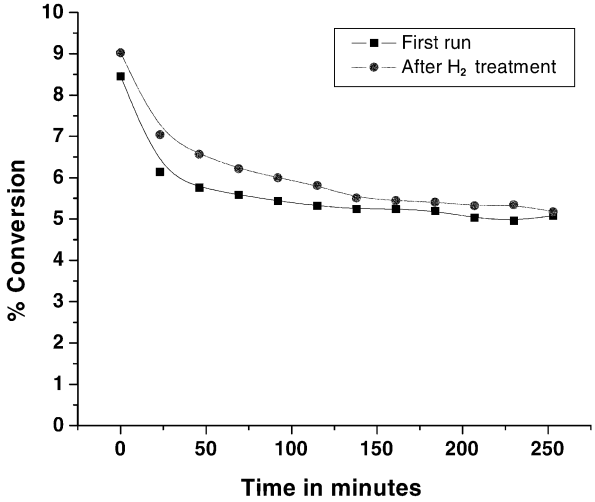

Figure 9. CO oxidation activity of 1 wt% Au/Al_2O_3 catalyst (sintered at 600 °C for 0 h) at room temperature. The initial deactivation of this catalyst is reversible, regeneration by H_2 at room temperature can restore activity.

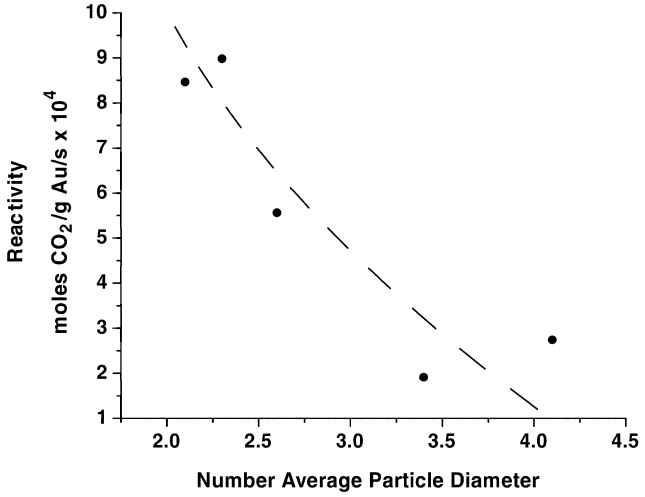

Figure 10. Effect of particle diameter on CO oxidation rate.

Alternatively, if the catalyst activity was located exclusively at the perimeter, activity should scale as $1/(D_p)^2$, where D_p is the perimeter average diameter. When we plot the data, we find that the fit is reasonably good for both models; therefore, within the limits of error, we cannot discriminate between these two competing models for the reactivity of Au catalysts.

4. Discussion

In this paper we have demonstrated a novel approach for the preparation of highly dispersed Au catalysts via impregnation under acidic conditions from the $HAuCl_4$ precursor. The reactivity of these catalysts is reported in table 1 in units of moles CO_2/g Au/s and also as a turnover frequency. The TOF is based on a value of dispersion that is calculated from the surface average diameter, as explained in the experimental section. It can be seen that the TOF values on these catalysts at room temperature are comparable to the catalysts reported in the literature [8]. Our work was performed under nearly stoichiometric conditions at a higher absolute pressure of reactants ($P_{CO} = 16.7$ kPa and $P_{O_2} = 8.6$ kPa). The different reaction conditions must be considered when comparing these reactivity results. For example, the recent work of Costello *et al.* [8] reports a TOF of 0.17–0.46 on their most active catalyst, but at a lower absolute pressure of reactants ($P_{CO} = 1$ kPa and $P_{O_2} = 2.5$ kPa) and under net oxidizing conditions.

This study shows that the impregnation route can yield catalysts that have CO oxidation reactivity comparable to the catalysts prepared by other techniques such as deposition–precipitation. The key feature in our approach is that we adsorb the Au precursor at its saturation coverage. At low pH, the alumina is positively charged and is able to adsorb the $(AuCl_4)^-$ anions. We have confirmed that the Au precursor is irreversibly adsorbed and cannot be washed off in water at pH 7. Analysis of the filtrate shows the presence of Cl^- anions suggesting that the support is acting as a ligand and exchanging hydroxyl groups for the Cl^- ions which are released from the Au chloride precursor. Subsequent treatment with a strong base, after washing off excess $(AuCl_4)^-$, leads to hydrolysis of the anion complex to release the remaining chloride anions and to convert the Au into the hydroxide form. The released chloride can be easily washed off yielding an adsorbed Au complex that can be decomposed at low temperatures (as low as 150 °C) to yield active Au catalysts. The decomposition temperature determines the overall particle size distribution. Eliminating the chloride anion appears to be important for obtaining catalysts with high activity, as pointed out by Oh *et al.* [5] who show that chloride is not only a poison for Au catalysts but it also accelerates the sintering of Au catalysts.

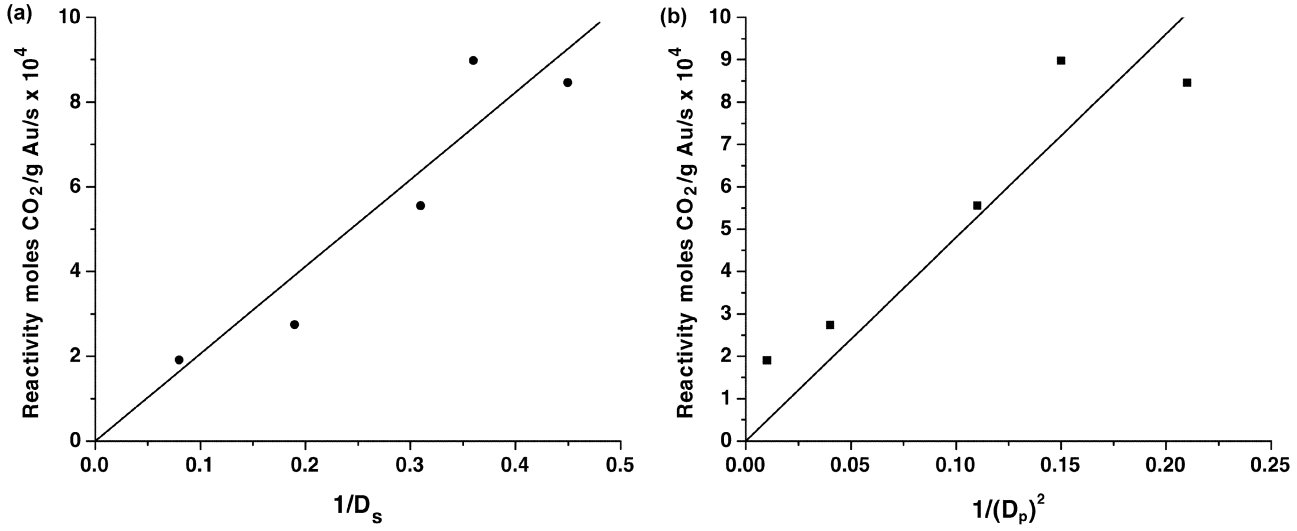

Figure 11. Test for the perimeter and surface model for reactivity: (a) reactivity versus $1/D_s$ (surface area per gram); (b) reactivity versus $1/(D_p)^2$ (perimeter length per gram).

The catalysts prepared by our impregnation route are hydrothermally stable, calcining them in a 10 mol% H_2O stream at 600 °C for 96 h causes the mean diameter to increase to about 4 nm. We have compared the sintering behavior of Au with Pd at similar Tamman temperature, $T_{\text{sintering}}/T_{\text{melting}}$. At a Tamman temperature of 0.6, we have sintered Au ($T_{\text{sintering}} = 600\,^{\circ}\text{C}$) and Pd ($T_{\text{sintering}} = 900\,^{\circ}\text{C}$) catalysts in an atmosphere containing 10% H_2O for 96 h, and we find that while Pd reaches a particle size of 25 nm [7], Au has sintered to only 4 nm. The hydrothermal stability of these Au catalysts suggests that they may have potential for applications in automotive exhaust catalysis for achieving light off at low temperatures.

The sintering experiments have provided us with a number of catalysts with differing crystallite sizes. In addition, we varied the metal loading by modifying the preparation conditions, and this set of catalysts was used to investigate the effect of crystallite size on activity. Our data show that activity drops dramatically as the crystallite size reaches 4 nm, in agreement with the observations of Haruta and Date [4], but we cannot discriminate between a model that presumes that all exposed Au atoms are reactive versus one where only the atoms at the perimeter are reactive. In order to address this question, we plan to expand the study to a wider range of particle diameters.

5. Conclusion

A novel approach based on aqueous impregnation from a gold chloride precursor has been developed to prepare highly dispersed catalysts. These catalysts have low chloride content and excellent hydrothermal stability. The activity of these catalysts compares favorably with literature reports of catalysts prepared by the deposition–precipitation method.

Acknowledgments

Financial support for this work from the National Science Foundation, GOALI program, grant CTS-99-11174 and Delphicatalyst, Tulsa, OK, is gratefully acknowledged. The electron microscopy was performed in the microscopy facility in the Earth and Planetary Sciences Department. We acknowledge support for the TEM acquisition via NSF grant CTS 98-71292.

References

[1] R.J. Puddephatt, *The Chemistry of Gold* (Elsevier/North-Holland, Amsterdam, New York, 1978).
[2] M. Haruta, T. Kobayashi, H. Sano and N. Yamada, Chem. Lett. 2 (1987) 405.
[3] G.C. Bond and D.T. Thompson, Gold Bull. 33 (2000) 41.
[4] M. Haruta and M. Date, Appl. Catal. A: General 222 (2001) 427.
[5] H.S. Oh, J.H. Yang, C.K. Costello, Y.M. Wang, S.R. Bare, H.H. Kung and M.C. Kung, J. Catal. (in press).
[6] A.I. Kozlov, A.P. Kozlova, H.C. Liu and Y. Iwasawa, Appl. Catal. A: General 182 (1999) 9.
[7] Q. Xu, K.C.C. Kharas and A.K. Datye, Stud. Surf. Sci. Catal. 139 (2001) 157.
[8] C.K. Costello, M.C. Kung, H.S. Oh, Y.M. Wang and H.H. Kung, Appl. Catal. A: General 232 (2002) 159.